Digest Journal of Nanomaterials and Biostructures Vol. 6, No 3, July-September 2011, p. 1103-1110

MAGNETIC AND MAGNETO-TRANSPORT PROPERTIES OF GRANULAR [Ni-Fe/Zn/Co-Ni-N/Ni-Mn] SPIN VALVES

P. PASCARIU*, S.I. TANASE, D. TANASE, V. GEORGESCU
Faculty of Physics "Al. I. Cuza" University, Iaşi 700506, Romania

In this work, we report experimental results concerning the giant magnetoresistance effect and the magnetic properties of [Ni-Fe/Zn/Co-Ni-N/Ni-Mn] spin-valve sandwich electrodeposited on Cu substrate. The attraction of such granular spin valves is that they can be very easily manufactured, with a view to their application as magnetoresistive material in magnetic field sensors. The granular structure is induced both due to the immiscibility of the diamagnetic Zn layer with the ferromagnetic Co-Ni-N, and to the addition of N impurity in the Co-Ni-N layer. The thickness of the Zn diamagnetic interlayer (varying between 3 nm and 13 nm) plays a significant role on the magnitude of the giant magnetoresistance (GMR) effect, and the magnetic behavior is dependent on this parameter. The magnetoresistance measured in current in plane (CIP) and current perpendicular to plane (CPP) configurations, with dc magnetic field applied in the film plane, varied with Zn interlayer thickness, exhibiting a GMR contribution of about 13% (CIP) and 10% (CPP) in the case of [Ni-Fe(140nm)/Zn(3 nm)/Co-Ni-N(150nm)/Ni-Mn(160nm)] granular spin-valve stack.

(Received May 5, 2011; Accepted July 6, 2011)

Keywords: spin valve; electrodeposition; electronic transport; magnetic properties

1. Introduction

Since the discovery of the giant magnetoresistance (GMR) [1], multilayered structures consisting of ferromagnetic layers separated by a nonmagnetic spacer layer have been the focus of great attention. The spin valve structures first proposed by Dieny [2] were reported to be the most promising candidates for magnetic sensors and high-density read-out heads due to their low field switching properties and high sensitivities. Compared with sputtering and evaporation, which were most commonly used in the production of GMR materials, electrodeposition method exhibited its advantages of low cost, simplicity and ease of large-scale production.

Spin-valve structures have the advantage of high magnetoresistance (MR) signals and high sensitivities at lower fields, which are important considerations for many sensing applications, especially for the low field magnetic sensors. Generally, a spin valve is a simple multilayer structure with two ferromagnetic (FM) layers having different coercivity, separated by a thin nonmagnetic spacer layer. This difference in coercitivity can be achieved, for example, by having different layer thicknesses but a more controlled way is the pinning of one of the layers to an antiferromagnetic (AF) layer, leaving the other magnetic layer free to rotate [3-6]. In this case there is not a repetition of layers, and it is called therefore a sandwich. In our experiment we propose to obtain a spin valve structure composed from Ni-Fe (permalloy) as soft ferromagnetic layer, Zn as nonmagnetic layer, Co-Ni-N as hard ferromagnetic layer pinned to Ni-Mn as antiferromagnetic layer. For now, we have not found published results about electrodeposition and study of magnetic and transport properties of [Ni-Fe/Zn/Co-Ni-N/Ni-Mn] spin valves. The granular structure is induced in such a sandwich both due the immiscibility of the diamagnetic Zn

*Corresponding author : pascariu_petronela@yahoo.com

layer with the ferromagnetic Co-Ni-N and to preferentially localized N impurity at the granules frontiers added in Co-Ni-N layer.

In this work, we describe in brief the procedure of preparation of [Ni-Fe/Zn/Co-Ni-N/Ni-Mn] spin valve films by electrodeposition on Cu substrate. We studied the effects of the Zn layer thickness concerning the magnetic and magneto-transport properties of spin valve stack, with a view to find possible technological applications.

2. Experimental

A spin valve film in our work consists of four metal layers: an antiferromagnetic pinning layer (Ni-Mn), a pinned layer (Co-Ni-N) whose magnetization is fixed by an exchange-coupling field from the antiferromagnetic layer, a Zn diamagnetic interlayer, and a free layer (Ni-Fe with permalloy composition) whose magnetization rotates according to the applied magnetic field. Generally, the electrical resistance of the spin-valve film should be low when magnetizations from the pinned layer and free layer are parallel and high when they are antiparallel.

The [Ni-Fe/Zn/Co-Ni-N/Ni-Mn] spin valves were electroplated on the surface of a disk-shaped cathode (20 mm diameter) made of cfc (100)-textured polycrystalline copper foils. Electrodeposition was performed in potentiostatic regime, using a holder system containing three electrodes, namely: cathode, a platinum anode and a platinum wire as quasi-reference electrode (the contact area with solution was of 0.06 mm^2). The system of electrodes was successively introduced in four principal baths for component layers electrodeposition, controlling the time of immersion; before each immersion in electrolytic baths, and after the final layer deposition, the system was carefully rinsed in distilled water. The copper substrates were surfaced prior to electroplating by abrasion with emery powder, etching in dilute HNO_3, and washing in distilled water. In this work, the electrodeposition was carried out in four separate baths. The first bath contained 6 g/l $FeSO_4\cdot 7H_2O$, 218 g/l $NiSO_4\cdot 7H_2O$, 25 g/l H_3BO_3, 25 g/l NaCl and additive solution for plating a permalloy ($Ni_{80}Fe_{20}$) layer, using the preparation recipe from [7, 8]. The second bath contained 40 g/l $ZnSO_4\cdot 7H_2O$, 20 g/l $(CH_3COO)_2$ $Zn\cdot 2H_2O$, and the additional substances (30 g/l H_3BO_3, 40 g/l NaCl, 40 g/l $Na_2SO_4\cdot 10H_2O$, 0.8 ml/l $C_6H_{15}NO_3$) for plating Zn spacer layer, with composition and parameters originally established from our experiments [9]. The third bath contained 30 g/l $CoSO_4\cdot 7H_2O$, 50 g/l $NiSO_4\cdot 7H_2O$, 10 g/l $NiCl_2\cdot 6H_2O$, 50 g/l $Na_2SO_4\cdot 10H_2O$, 30 g/l H_3BO_3, 10 g/l NaCl, 0.8 g/l sodium laurylsulphate ($C_{12}H_{25}NaO_4S$), 4 g/l sodium saccharine ($NaC_7H_4O_3NS\cdot 2H_2O$), and 1 g/l sodium nitrate ($NaNO_3$) used as a source for nitrogen inclusion in the films. The solution composition and electrodeposition parameters were the same as those described in our previous papers [10, 11]. The fourth bath contained 2g/l $NiSO_4\cdot 7H_2O$, 150 g/l $MnSO_4\cdot H_2O$ and 50 g/l $(NH_4)_2SO_4$ for plating Ni-Mn, electrodeposition being performed as in the paper [12]. In a view to simplify the deposition procedure, electrodeposition was carried out at 3.0 V bias voltages for all electrolytic baths, without stirring the electrolyte, by introducing the holder system of electrodes in the four deposition solutions and the intermediate washing water baths.

The thickness for the Ni-Fe, Co-Ni-N and Ni-Mn layers were controlled by the electric charge passing through the electrolyte, and the rate of electrodeposition. The rate of electrodeposition for each layer composing the spin valve was established by depositing a thick (500 nm) film of that layer in the same conditions as those used for spin valve electrodeposition. The weights of the deposits were measured for these thick films by means of a microbalance with an error of $\pm 10^{-6}$ g. In addition, a MII-4 Linnik interferential microscope was used to measure the thickness of these films by the multiple-beam Fizeau fringe method, at reflection of monochromatic light. For the Zn layer medium thickness calculation we used Faraday law of electrodeposition. The deposition rates of Ni-Fe, Zn, Co-Ni-N and Ni-Mn layers were estimated as 0.5 nm/s, 0.7 nm/s, 0.3 nm/s and 0.5 nm/s, respectively. We mention that in the case of granular films composed of granules with various diameters, the thickness of different layers is estimated only as a medium thickness, but the studies on this subject are out of the focus of the present work.

The morphology and compositional investigation of the samples were made with a scanning electron microscope (SEM), model Vega II LSH, coupled with a detector EDX, model Quantax QX2. This detector is used for the quantitative and qualitative microanalysis of the thin films using MnK_α radiation. The magnetic measurements were carried out using an induction type device with the *ac* magnetic field applied in the film plane (50 Hz, in a maximum field of 750 *Oe*), at room temperature.

The measurements of the film resistance (*R*) were carried out with an HM 8112-2 programmable multimeter, with the conventional four-point-in-line method both for current in plane (CIP), and for current perpendicular to the film plane (CPP) configurations, for applied magnetic fields up to ± 650 Oe.

The magnetoresistance was defined as:

$$MR = \frac{R_0 - R_S}{R_S} \times 100\%,$$

in which R_0 is the film resistance measured in the absence of an applied magnetic field and R_s is the resistance in the maximum positive applied magnetic field.

3. Results and discussion

From our previous preliminary experiments, we established the electrodeposition conditions and the optimal thickness for soft and hard ferromagnetic layers, and for antiferromagnetic layer, in a view to obtain a magnetic hysteresis cycle with specific shape of spin valve structures. The ferromagnetic layers are permalloy (80.0 at% Ni, 20.0 at% Fe) and 79.5 at% Co, 19.2 at% Ni, 1.3 at% N_2. The non-magnetic spacer layer is Zn and the antiferromagnetic layer employed is equiatomic NiMn. In this work, we study the influence of the Zn diamagnetic spacer on the magnetic and magneto-transport properties of the spin valve samples. We prepared a series of [Ni-Fe/Zn/Co-Ni-N/Ni-Mn] samples with varied Zn layer thickness (t_{Zn}), as follows: S1 (t_{Zn}=3 nm), S2 (t_{Zn}=6 nm), (t_{Zn}=10 nm) and (t_{Zn}=13 nm), respectively. The thicknesses of the Ni-Fe, Co-Ni-N and Ni-Mn layers in spin valve structures were maintained constant, at t_{NiFe} = 140 nm, $t_{Co\text{-}Ni\text{-}N}$ = 150 nm and $t_{Ni\text{-}Mn}$ = 160 nm for all the samples.

It is known that the critical length scales in granular systems are the particle diameter, analogous to the thickness of the ferromagnetic layer, and the inter-particle separation, analogous to the thickness of the non-magnetic layer [13]. Also, the particles must also be small enough to be single domain. Although our spin valve stacks are formed from layers with relatively large medium thickness, they are composed from granules with diameters in the nanometer range.

For all the samples we obtained the morphology of granular type. As a representative example we present in figure 1 the scanning electron micrographs of the surface topography of the sample S1 (at 20 μm and 10 μm length scale, in left and right side figures, respectively). The SEM images show that the samples are composed from a mixture of grains with various diameters grown onto copper substrate. We can notice that the granular stack develop by a Volmer –Weber mechanism; the existence of grains with varied diameters proves the growth mechanism of the films by progressive nucleation. More systematic studies are still needed in order to reveal which microstructural features are really decisive in affecting the GMR magnitude. The granular structure and interface quality is certainly one of these factors and we will try to get further information on the interfaces in electrodeposited spin valves by appropriate TEM and XRD techniques.

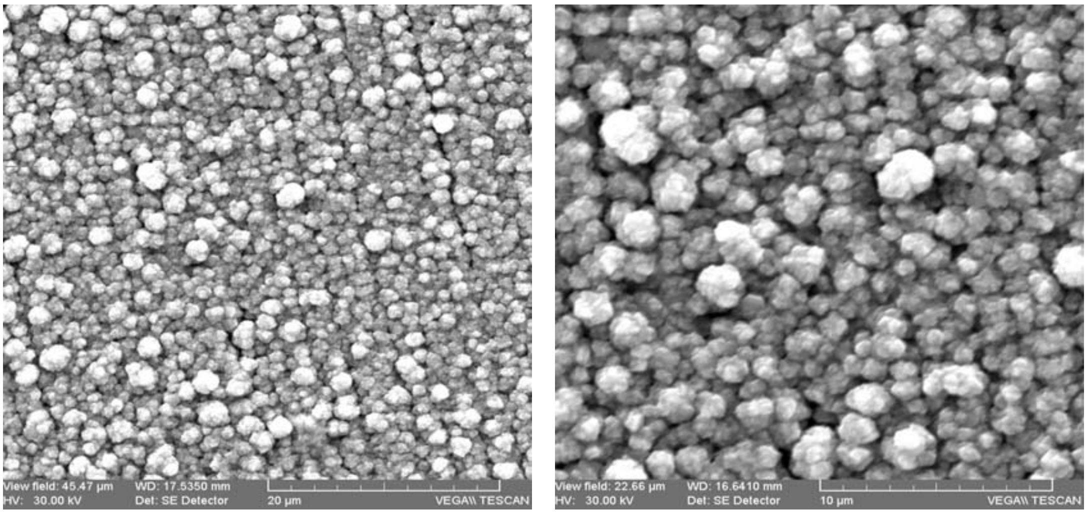

Fig.1. SEM images of [Ni-Fe/Zn/Co-Ni-N/Ni-Mn] spin valve for the sample S1 (length scale 20 µm in left side figure and 10 µm for the right side figure).

Fig. 2 shows the magnetic hysteresis loops (a, b) and magnetic susceptibility curves (c, d) registered for the samples S1 and S4, having the Zn layer thickness of 3 nm and 13 nm, respectively. The two-step magnetic hysteresis curve in figures 2a and 2b (and correspondingly two-step susceptibility curves from figures 2c and 2d) suggest that the magnetizations of Ni-Fe and Co-Ni-N magnetic layers reverse almost independently. It is seen in these figures that we achieved well defined switching of the Co-Ni-N and Ni-Fe (permalloy) layers. When a magnetic field larger than anisotropy field (H_k) is applied, both the permalloy and Co-Ni-N align in the same direction and we obtain a high net magnetic moment. When the applied field is decreased to zero both permalloy and Co-Ni-N are still magnetized in one direction. When the field is reversed and increased above the coercive field of the permalloy layer, the permalloy layer switches to the opposite direction and we obtain a low net magnetization. In this state the magnetization of the Co-Ni-N and permalloy layers are aligned opposite to each other. When we again increase the applied field in the negative direction and when the applied field is greater than the coercive field of the Co-Ni-N layer, the Co-Ni-N magnetization also switches in the applied field direction. Again both the permalloy and Co-Ni-N magnetizations are aligned parallel to each other and we obtain a higher net magnetization.

Coercive fields H_{c1} and H_{c2} of the two ferromagnetic layers were determined as the magnetic fields corresponding to the two maximum values in susceptibility curves. For the sample S1, the magnetization of the softer component (Ni-Fe) layer reverses abruptly in a lower external field (coercive field is $H_{c1} \approx 68$ Oe). A larger external field is required to reverse the magnetization of the harder (Co-Ni-N) layer ($H_{c2} \approx 319$ Oe*)*. The coercivity fields of the sample S4 (figure 2.d) are of about $H_{c1} \approx$ *86 Oe* and $H_{c2} \approx 337$ *Oe*. The remanence ratio of S1 (t_{Zn}=3 nm) is of about $M_r/M_s \approx 0.57$. For the sample S4 (t_{Zn}=13 nm) the remanence is $M_r/M_s \approx 0.61$. The anisotropy fields for the two samples (S1 and S4) are of about 593 Oe and 480 Oe, respectively.

The switching field distribution SFD=$\Delta H/H_c$, where ΔH is the full width at half maximum of the differential susceptibility χ=dM/dH, near H_c is a measure of the transition fluctuations, that could be very important for granular films. We obtained for the sample S1 the SFD of maximum value (SFD = 0.77) at H_{C1} = 68 Oe and of minimum value (SFD = 0.46) at H_{C2} = 319 Oe, respectively. The SFD for the sample S4 are of about 0.47 at H_{C1} = 88 Oe and 0.51 at H_{C2} = 337 Oe. The smeared curves of magnetic susceptibility from figure 2c and figure 2d indicate a broad grain size distribution, but interactions between the grains are also likely to play a role as the Zn layer thickness increases (in the case of the S4 sample).

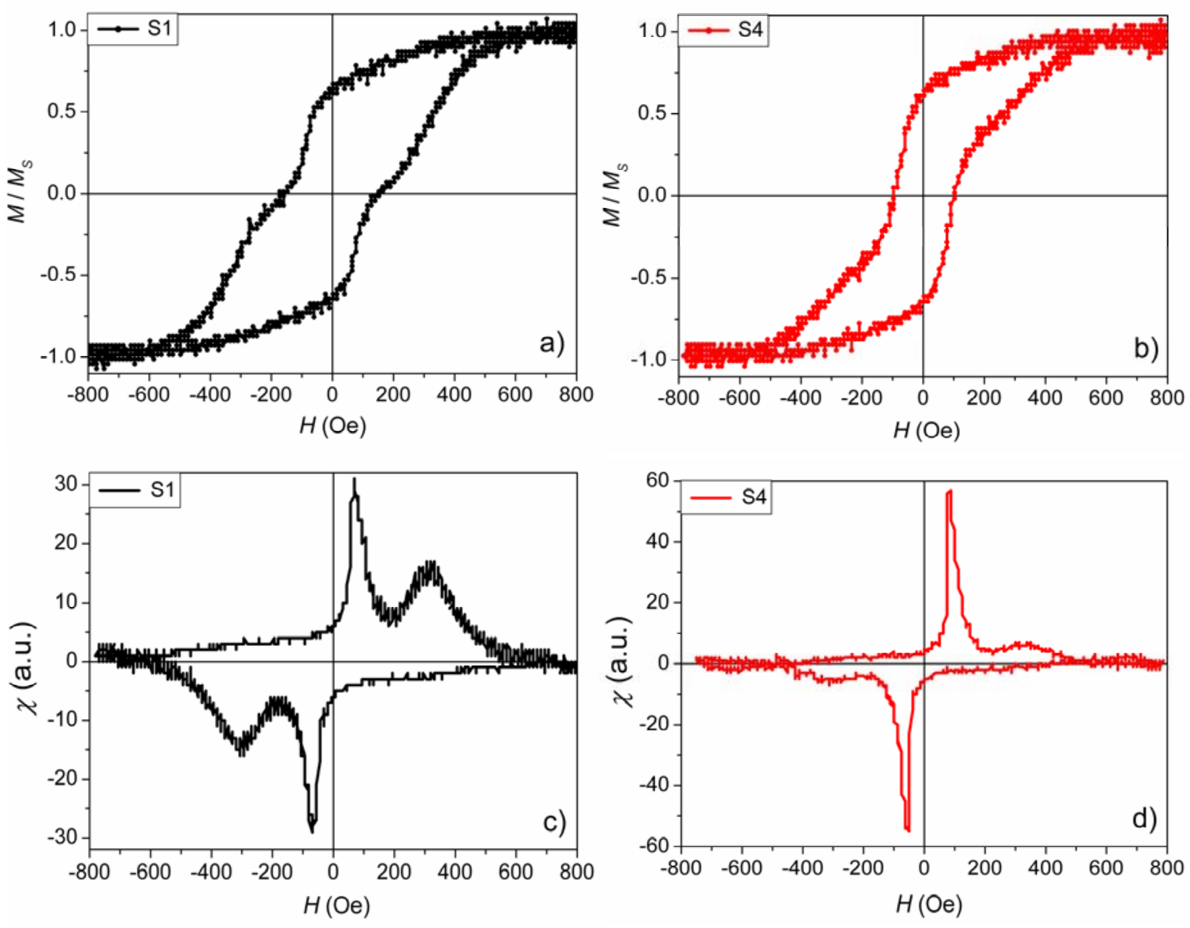

Fig. 2. Comparison between hysteresis loops (a, b) and magnetic susceptibility curves (c, d) of the samples S1 and S4 (from [Ni-Fe/Zn/Co-Ni-N/Ni-Mn] spin valves) with t_{Zn}=3 nm, and t_{Zn}=13 nm, respectively.

The magnetic susceptibility curves in (figure 2c and figure 2d) as the hysteresis cycles (2a, 2b) show a typical two staged magnetization reversal, which is indicative of the rather weak coupling between Ni-Fe and Co-Ni-N layers, especially in the case of the sample S1. When t_{Zn}=13 nm, the reversal process of Ni-Fe and Co-Ni-N layers is more difficult due to the interlayer or inter-grains exchange coupling, which is confirmed by the corresponding hysteresis loop with an indistinct step in figure 2b. We may conclude from these experiments that, by keeping in the spin valve structure the same thickness of the Ni-Fe, Co-Ni-N and Ni-Mn layers (t_{Ni-Fe}=140 nm, $t_{Co-Ni-N}$=150 nm, t_{Ni-Mn}=160 nm), the magnetic behavior is dependent on the Zn layer thickness.

We will in brief present in the following results on the measurements of the magnetoresistance. The dc magnetic field (with 750 Oe maximum value, larger than H_k) was applied in the film plane, either perpendicular to the current (in so called transversal CIP configuration), or parallel to the current (in longitudinal CIP configuration).

The magnetoresistance curves as a function of the applied magnetic field are shown in Fig. 4 for the samples S1 (*a* and *b*) and S4 (c and d). The graphs from fig. 4a, and 4c are recorded in current in plane configuration, with in plane applied magnetic field, parallel to current (so called CIP longitudinal configuration), and those from figures 4b and 4d correspond to CIP transversal configuration with in plane applied magnetic field, perpendicular to current.

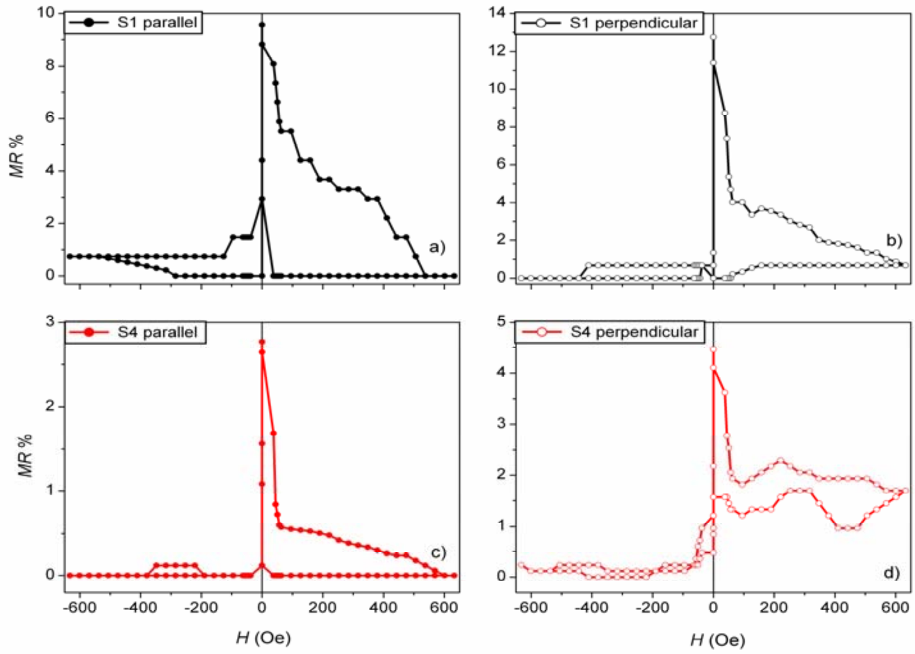

Fig. 4. Magnetoresistance (MR) of samples S1 and S4 as a function of the applied in plane magnetic field H, measured in: CIP longitudinal configuration (a, c) and CIP transversal configuration (b, d).

The curves of figure 4 exhibit a very sharp rise corresponding to the switching of the free layer. The largest value of GMR we achieved is 13% at room temperature for the sample S1. The amplitude of the transition offer possibilities for technological applications in flux-sensing devices [14]. One could see from these curves that the increase of the Zn spacer layer thickness from 3 to 13 nm was found to increase the values of MR for the samples.

The variation of giant magnetoresistance with the in plane applied magnetic field, for the samples S1 and S4, are presented in figure 5 with the current direction perpendicular to the plane of thin film (CPP configuration).

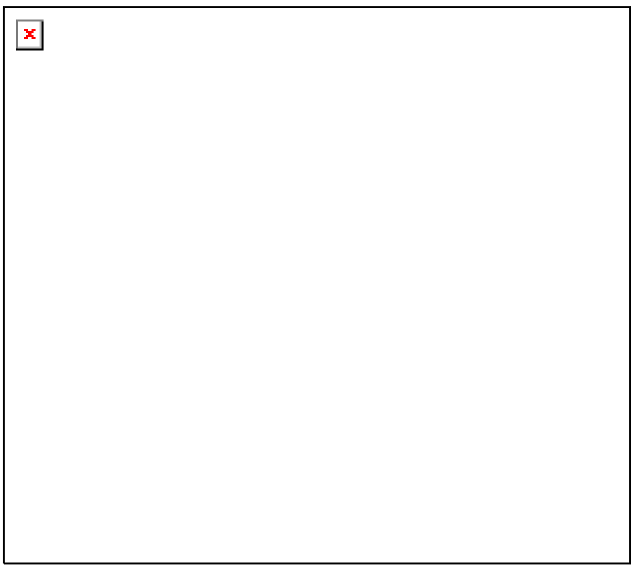

Fig. 5. Magnetoresistance (MR) of samples S1 and S4 as a function of applied in plane magnetic field H (Oe) with the current direction perpendicular to the plane of thin film (CPP)

The shapes of *MR(H)* curves in figures 4 and 5 are similar with other experiments on spin valves stacks with a structure like: FM/NM/FM/AF, where FM is a ferromagnet, NM a non-magnetic spacer layer and AF layer an antiferromagnet. Such four layer systems were firstly reported by Dieny [15]. In the [Ni-Fe/Zn/Co-Ni-N/Ni-Mn] stacks, the Ni-Mn pins the upper Co-Ni-N layer, and does not rotate at low fields (the antiferromagnet has no net magnetic moment). The resulting hysteresis loop and magnetoresistive behaviour are shown in Figs. 2a, b and 4, 5, respectively. In this case the soft layer rotates at low field and the pinned layer turns at large field, but flips back to its pinned position if the field becomes smaller again. The largest values for the giant magnetoresistance contribution were of 13% for the Zn layer thickness t_{Zn}= 3 nm (sample S1) and of about 10% for the samples S4 with t_{Zn}= 13 nm, respectively. An overview of the determined magnetic and magneto-transport properties of all samples is given in Table I.

Table I. Measured values of the coercive fields H_{c1}, H_{c2}, the remanence ratio M_r/M_S and the anisotropy field H_k.

Sample	t_{Zn} (nm)	H_{C1} (Oe)	H_{C2} (Oe)	M_r/M_S	H_k (Oe)
S1	3	68	319	0.57	593
S2	6	74	325	0.58	538
S3	10	80	337	0.59	490
S4	13	86	337	0.61	480

It is found that the coercivity fields H_{c1}, H_{c2}, anisotropy field H_k and the remanence ratio M_r/M_s increase when the Zn layer thickness is increased. We suppose that the thinnest Zn film has no exchange bias, but as the Zn layer thickness increases to 13 nm, the locally formed exchange bias develops. Likewise, the coercivities increase with increasing Zn layer thickness. This behavior is similar to that seen in other exchange bias systems [14]. The magnetoresistance values varied with the Zn layer thickness. The giant magnetoresistance contribution was of 13% for the Zn layer thickness t_{Zn}=3 nm (sample S1) and of about 9% for the samples with the Zn layer t_{Zn}=13 nm (samples S4), respectively.

We are trying to explain these results. In case of a Zn spacer layer which is thicker than the mean free path of the conduction electrons, the electrons are able to move through this layer, or through the Zn layer and one magnetic layer, without crossing two magnetic layers. Changing orientation of the magnetic layers by applying a magnetic field will not induce a change in resistance for these electrons. Besides this, the antiferromagnetic coupling also decreases with increase of spacer layer thickness. The results depend strongly on whether the MR is due to spin-dependent bulk scattering or spin-dependent interface scattering. Theoretical calculations [16] (which show excellent agreement with experimental results) for the Fe/Cr system indicate that about 65-75% of the MR arises from scattering at the interfaces. In contrast, $Ni_{80}Fe_{20}$/Cu multilayers have been analyzed within a picture where bulk scattering is dominant [17], for CIP. However, for CPP the relative contributions differ. Taking into account this complex picture of the phenomenon, we consider that the MR in [Ni-Fe/Zn/Co-Ni-N/Ni-Mn] spin valve stacks is mostly due to spin dependent grain-matrix interface scattering and to a lesser extent, from spin dependent scattering within the magnetic grains.

4. Conclusions

The present work discusses the electrodeposition of [Ni-Fe/Zn/Co-Ni-N/Ni-Mn] spin valve stacks, exhibiting appreciable GMR of 2.7 ÷ 13% at room temperature. The spin valve stacks were deposited from four sulfate bath solutions by separate baths procedure. Using the control of the electrodeposition chemistry, *pH*, current density and temperature, [Ni-Fe/Zn/Co-Ni-N/Ni-Mn] spin valves with good magnetic properties were obtained.

Comparing the shapes of the hysteresis loops, we have found that the magnetic features are very different, depending on the Zn layer thickness. It was shown for the first time that the combination of [soft magnetic /diamagnetic/hard magnetic/antiferomagnetic] layers with Zn as diamagnetic and Co-Ni-N as hard ferromagnetic layers showed the GMR effect.

The effect of individual Zn layer on the magnitude and behavior of GMR has been studied. By varying the thickness of Zn layer, the coercive fields corresponding to free and pinned layers varied in the range 68 Oe÷ 86 Oe for Ni-Fe layer and 319 Oe ÷ 337 Oe for the Co-Ni-N layer. It was observed that for lower thicknesses of Zn layer, the GMR ratio has the best values both for CIP and CPP configurations. The Zn layer thickness seems to control the nature of magnetic coupling and spin dependent grain-matrix interface scattering of electrons, with the two showing a correlation.

Acknowledgement

This work was partially supported by the Ministry of Education, Research, Youth and Sport and by the Social European Funds provided through Project 5244 No. RO08- POSDRU-6/1.5/S/25.

References

[1] M. N. Baibich, J. M. Broto, A. Fert, Van Dau F. Nguyen, F. Petroff, P. Etienne, G. Creuzet, A. Friederich, V. Chazelas, Phys. Rev. Lett. **61***,* 2472 (1988).
[2] B. Dieny, V. S. Speriosu, S. S. P. Parkin, B. A. Guiney, D. R. Wilhat, D. Mauri, Phys. Rev. B **43**, 1297-1300 (1991).
[3] H. Wang, Y. Wu, Q. Li, M. Wang, G. Li, L. Zhang, Appl. Phys. Lett*.* **89**, 052107 (2006).
[4] B. Szymański, F. Stobiecki, T. Luciński and K. Röll, Czechoslovak Journal of Physics **52**, 235-238 (2002).
[5] Y. Jiang, S. Yao, W. Zhang, Thin Solid Films **516,** 3210–3216 (2008).
[6] X. L. Tang, H. W. Zhang, H. Su, Z. Y. Zhong, Y. L. Jing, J. Phys. D: Appl. Phys. **39,** 5121–5123 (2006).
[7] H. Chiriac, T. A. Óvári, and P. Pascariu, J. Appl. Phys. **103**, 07D919 (2008).
[8] N. Lupu, H. Chiriac, and P. Pascariu, J. Appl. Phys. **103**, 07B511 (2008).
[9] L. Vlad, P. Pascariu, S.I. Tanase, D. Pinzaru, M. Dobromir, V. Nica and V. Georgescu, Physica B, 10.1016/j.physb.2011.01.052
[10] C. Sirbu, V. Georgescu, J. Optoelectron. Adv. Mater. **10 (9)**, 2396–2401 (2008).
[11] S.I. Tanase, D. Tanase, P. Pascariu, L. Vlad, A.V. Sandu, V. Georgescu, Materials Science and Engineering B **167,** 119–123 (2010).
[12] A. Stephen, M. V. Ananth, V. Ravichandran and B. R. V. Narashiman, Journal of Applied Electrochemistry **30**, 1313-1316 (2000).
[13] S. M. Thompson, J. Phys. D: Appl. Phys. **41**, 093001 (2008).
[14] H. C. Wu, S. K. Arora, O. N. Mryasov, I. V. Shvets, Appl. Phys. Lett. **92**, 182502 (2008).
[15] B. Dieny, J. Magn. Magn. Mater. **136**, 335-359, (1994).
[16] P. M. Levy, S. Zhang and A. Fert, Phys. Rev. Lett*.* **65**, 1643 (1990).
[17] B. Dieny, Europhys Lett*.* **14**, 261-267 (1992).